Inorganica Chimica Acta, 197 (1992) 9–14

Mixed-valence complexes containing the Rh_2^{5+} core. X-ray crystal structure of the dimer-of-dimers $[Rh_2(form)_2(O_2CCF_3)_3(AgO_2CCF_3)_2]_2$ (form = *N,N'*-di-*p*-tolylformamidinate anion)

Giuseppe Bruno*, Giuseppe Tresoldi, Sandra Lo Schiavo, Sergio Sergi
and Pasquale Piraino*
Dipartimento di Chimica Inorganica e Struttura Molecolare, Università di Messina, Salita Sperone no. 31, 98166 Vill. S. Agata, Messina (Italy)

(Received March 10, 1992)

Abstract

The chemical oxidation of the Rh_2^{4+} formamidinate derivative $Rh_2(form)_2(O_2CCF_3)_2(H_2O)_2$ (form = *N,N'*-di-*p*-tolylformamidinate) with the appropriate silver salt leads to the formation of the paramagnetic complexes $[Rh_2(form)_2(O_2CCF_3)_3(AgO_2CCF_3)_2]_2$ (**1**), $[Rh_2(form)_2(O_2CCF_3)_2(H_2O)_2]ClO_4$ (**2**) and $[Rh_2(form)_2(O_2CCF_3)](NO_3)_2$ (**3**). The complexes were characterized by EPR spectroscopy and X-ray analysis. The EPR spectra in frozen solution consist of two absorption lines. The low-field one is unresolved while the high-field one is split into a triplet. The pattern is interpreted in terms of hyperfine magnetic interaction between the unpaired electron and two equivalent ^{103}Rh nuclei ($I = 1/2$). Complex **1**, which consists of two $Rh_2(form)_2(O_2CCF_3)_3$ radicals axially linked by CF_3COOAg molecules, crystallizes in the monoclinic space group *C*2/*c*, with $a = 32.981(4)$, $b = 16.286(2)$, $c = 18.642(3)$ Å, $\beta = 94.32(4)°$, $V = 9984.3(4)$ Å^3, $Z = 4$ and $D_{calc} = 1.92$ g cm^{-3}.

Introduction

While a large number of dirhodium(II,II) compounds are known [1], complexes characterized by the presence of the Rh_2^{5+} core are much less common very likely due to the lack of general synthetic routes. For the most part these species have been detected by electrochemical methods and EPR spectroscopy [2], while up to now only few dirhodium(II,III) have been isolated and structurally characterized. These examples include $[Rh_2(O_2CCH_3)_4(H_2O)_2]ClO_4$, obtained via chemical oxidation of $Rh_2(O_2CCH_3)_4$ with ceric ions in sulfuric acid [3]; $[Rh_2(CH_3CONH)_4(theophylline)_2]NO_3$, obtained via chemical oxidation of $Rh_2(CH_3CONH)_4(theophillyne)_2$ with nitric acid [4]; Rh_2(2-anilinopyridine)$_4$Cl, obtained by reacting $Rh_2(O_2CCH_3)_4$ with an excess of 2-anilinopyridine [5]; and $[Rh_2(dpf)_4CH_3CN]ClO_4$ (dpf = *N,N'*-diphenylformamidinate), recently obtained by bulk-electrolysis at 0.65 V of the complex $Rh_2(dpf)_4$ [6].

Recently we reported a synthetic method that enabled us to synthesize the mixed-valence complexes $[Rh_2(form)_4]X$ ($X = NO_3$, O_2CCF_3; form = *N,N'*-di-*p*-tolylformamidinate) containing the Rh_2^{5+} core [7]. This method is based on the chemical oxidation with silver salts of the Rh_2^{4+} complex $Rh_2(form)_4$ and shows that silver ions allow the thermodynamic access to mixed-valence dirhodium(II,III) complexes when the oxidation potential of the corresponding dirhodium(II,II) derivatives does not exceed +0.25 V versus SCE.

As an extension of the previous work we report here the synthesis and EPR features of the new Rh_2^{5+} mixed-valence complexes $[Rh_2(form)_2(O_2CCF_3)_3(AgO_2CCF_3)_2]_2$ (**1**), $[Rh_2(form)_2(O_2CCF_3)_2(H_2O)_2]ClO_4$ (**2**) and $Rh_2(form)_2(NO_3)_2(O_2CCF_3)$ (**3**) obtained by chemical oxidation of the mixed-ligand Rh_2^{4+} complex $Rh_2(\mu\text{-form})_2(\mu\text{-}O_2CCF_3)_2(H_2O)_2$ with the appropriate silver salts. We report also the X-ray analysis of the unexpected complex **1** which provides the first example of a tetramer containing two Rh_2^{5+} radicals.

Experimental

The complex $Rh_2(\mu\text{-form})_2(\mu\text{-}O_2CCF_3)_2(H_2O)_2$ was prepared according to a literature procedure [8]. Other reagents and solvents were used as received. IR spectra were recorded on a Perkin-Elmer FT 43 instrument. EPR spectra were recorded by using a Bruker SR 200D

---

*Authors to whom correspondence should be addressed.

0020-1693/92/$5.00

spectrometer. Elemental analyses were performed by the Microanalytical Laboratory of the Organic Chemistry Institute of Milan and Analitische Laboratorien Malissa and Reuter, Elbach, FRG. The reactions were carried out either under a purified N_2 atmosphere or in air.

Synthesis of [$Rh_2(form)_2(O_2CCF_3)_3(AgO_2CCF_3)_2]_2$ (1)

To a dichloromethane solution of $Rh_2(form)_2(O_2CCF_3)_2(H_2O)_2$ (0.2 g, 0.21 mmol) was added solid AgO_2CCF_3 (141.1 mg, 0.63 mmol). After stirring for 3 h at room temperature the resulting royal blue mixture was filtered through Celite to remove metallic silver. Evaporation of the volatiles gave complex **1**, which was isolated as well formed crystals by slow evaporation of the solvent from a $CHCl_3$/n-heptane mixture. Yield 51%. IR spectrum (KBr pellet, cm^{-1}): $\nu_{asym}(CO_2)$ 1610, 1655. EPR spectrum (CH_2Cl_2, 100 K): $G_{\|}=1.937$, $A_{\|}=22\times10^{-4}$ cm^{-1}.

Synthesis of [$Rh_2(form)_2(O_2CCF_3)_2(H_2O)_2]ClO_4$ (2)

0.2 g (0.21 mmol) of $Rh_2(form)_2(O_2CCF_3)_2(H_2O)_2$ was dissolved in CH_2Cl_2 (20 ml) and 45.19 mg (0.21 mmol) of crude $AgClO_4$ was added. In a few minutes a blue color appeared. After 1 h the solution was filtered through Celite and the resultant solution layered with n-heptane. Well formed crystals of **2** were collected after 5 days. Yield 72%. IR spectrum (KBr pellet, cm^{-1}): $\nu_{asym}(CO_2)$ 1622; $\nu_{asym}(H_2O)$ 3620(w), $\nu_{sym}(H_2O)$ 3530(w). Molar conductivity (Ω^{-1} cm^2 M^{-1}): λ 165 (CH_2Cl_2, 10^{-3} M). EPR spectrum (CH_2Cl_2, 100 K): $G_{\|}=1.964$, $A_{\|}=20\times10^{-4}$ cm^{-1}.

Synthesis of $Rh_2(form)_2(NO_3)_2(O_2CCF_3)$ (3)

$Rh_2(form)_2(O_2CCF_3)_2(H_2O)_2$ (0.15 g, 0.16 mmol) in CH_2Cl_2 was allowed to react with $AgNO_3$ (59.1 mg, 0.35 mmol) dissolved in a mixture of CH_3OH/H_2O (3:1). After 3 h the blue solution was filtered and the volatiles removed *in vacuo*. The residue compound was extracted with several portions of diethyl ether leaving a residue which, after crystallization from CH_2Cl_2/n-heptane, gave complex **3** as blue needles. Yield 48%. IR spectrum (KBr pellet, cm^{-1}): $\nu_{asym}(CO_2)$ 1610. EPR spectrum (CH_2Cl_2, 100 K): $G_{\|}=1.947$, $A_{\|}=21\times10^{-4}$ cm^{-1}.

X-ray data collection and structure refinement

Suitable blue–black crystals of **1** were obtained by slow evaporation of the solvent from a benzene–heptane solution. Diffraction measurements were made on a Siemens-Stoe four-circle diffractometer using graphite-monochromated Mo Kα ($\lambda=0.71073$ Å) radiation. Accurate unit-cell dimensions and crystal orientation matrices were obtained from least-squares refinement of 2θ, ω, χ and Ψ values of 25 strong reflections in the range $15<2\theta<30°$. Compound **1** crystallizes in the monoclinic space group *C*2/*c*, with $a=32.981(4)$, $b=16.286(2)$, $c=18.642(3)$ Å, $\beta=94.32(4)°$, $V=9984.3(4)$ Å^3, $Z=4$ and $D_{calc}=1.92$ g cm^{-3}. Lorentz and polarization corrections were applied to the intensity data but no absorption correction was made due to the low absorption coefficient ($\mu=15.1$ cm^{-1}) and the fairly uniform dimensions of the crystals. The structure was solved by using standard Patterson methods, successive least-squares refinements, and difference Fourier maps. The final residuals for 504 variables refined against the 3308 data for which $F^2>3\sigma(F^2)$ were $R=5.8\%$, $R_w=6.1\%$. Scattering factors for non-hydrogen atoms were taken from ref. 9 and for hydrogen atoms from ref. 10. Anomalous dispersion corrections for Rh and Ag atoms were taken from ref. 11. All calculations were performed with SHELX 76 [12] and PARST [13] set of programs on the IBM 4341 computer at the 'Centro di Calcolo dell'Università di Messina'.

Crystal and data refinement are given in Table 1. Table 2 lists the fractional atomic coordinates; Table 3 gives the bond distances and angles.

TABLE 1. Crystal and refinement data for complex **1**

Formula	$C_{80}H_{60}F_{30}N_8O_{20}Ag_4Rh_4\cdot H_2O$
Formula weight	2884.5
Crystal system	monoclinic
Space group	*C*2/*c*
a (Å)	32.981(4)
b (Å)	16.286(2)
c (Å)	18.642(3)
β (°)	94.32(4)
V (Å^3)	9984.3
Z	4
D_{calc} (g cm^{-3})	1.92
Crystal size (mm)	$0.12\times0.15\times0.15$
Orientation reflections: no., range (2θ)	25, $15<2\theta<28$
T (°C)	23
μ (cm^{-1})	15.1
radiation (Å)	Mo Kα, $\lambda=0.71073$
Monochromator	graphite crystal
Scan type	θ–2θ
Scan speed	variable
Scan range (°)	1.2
Standard reflections	3 measured after every 140 min
Data limits	$3<2\theta<50$
No. data collected	5120
Observed data	3308 ($I\geqslant\sigma(I)$)
No. parameters refined	504
R^a	0.058
$R_w{}^b$	0.061
Quality-of-fit indicator^c	1.39
Weighting scheme	$w=1.16537/(\sigma^2(F_0)+0.001052F_0{}^2)$
Largest shift e.s.d. in final cycle	0.95
Largest peak (e/Å^3)	0.66

[a] $R=[\Sigma|F_o|-|F_c|]/\Sigma|F_o|$. [b] $R_w[\Sigma w(|F_o|-|F_c|)^2/\Sigma w|F_o|^2]^{1/2}, w=n/(\sigma^2(F_o)$. [c] Quality-of-fit $=[\Sigma w(|F_o|-|F_c)^2/(N_{obs}-N_{param})]^{1/2}$.

TABLE 2. Fractional atomic coordinates for complex **1** with e.s.d.s in parentheses

Atom	*x*	*y*	*z*
Rh(1)	0.17662(4)	0.15227(8)	0.64836(7)
Rh(2)	0.11666(4)	0.23971(8)	0.62567(7)
Ag(1)	0.17172(5)	0.0216(1)	0.81761(9)
Ag(2)	0.04765(7)	0.2179(1)	0.7750(1)
F(13)	−0.0399(5)	0.375(2)	0.625(2)
O(9)	0.0147(8)	0.279(2)	0.692(2)
C(40)	0.028(1)	0.312(2)	0.640(2)
F(14)	−0.002(2)	0.401(3)	0.554(2)
F(15)	0.002(1)	0.468(2)	0.648(3)
C(41)	0.0016(6)	0.386(2)	0.628(2)
OW	0.421(1)	−0.009(3)	1.169(2)
F(4)	0.3025(4)	0.0078(9)	0.6536(9)
F(5)	0.3007(3)	−0.0565(8)	0.7523(7)
F(6)	0.3123(4)	0.071(1)	0.752(1)
F(10)	0.0328(6)	0.068(2)	0.914(2)
F(11)	0.0554(9)	0.172(1)	0.933(1)
F(12)	0.0733(8)	0.068(2)	0.986(1)
C(36)	0.2451(6)	0.030(1)	0.718(1)
C(37)	0.2900(7)	0.011(2)	0.720(1)
C(38)	0.0961(6)	0.082(1)	0.870(1)
C(39)	0.065(1)	0.099(2)	0.927(1)
O(5)	0.2280(4)	−0.0029(9)	0.7634(8)
O(6)	0.2322(3)	0.0800(7)	0.6724(7)
O(7)	0.1214(4)	0.0282(9)	0.8901(7)
O(8)	0.0937(4)	0.1260(8)	0.8183(7)
O(10)	0.0593(4)	0.313(1)	0.6157(9)
F(1)	0.0382(4)	0.0228(8)	0.7104(8)
F(2)	0.0659(5)	−0.042(1)	0.6282(8)
F(3)	0.0881(4)	−0.0490(8)	0.7342(8)
C(34)	0.0993(6)	0.077(1)	0.6714(9)
C(35)	0.0735(6)	0.004(1)	0.685(1)
O(1)	0.1374(3)	0.0594(6)	0.6787(6)
O(2)	0.0818(3)	0.1388(7)	0.6525(6)
N(1)	0.1678(4)	0.1114(8)	0.5489(7)
C(1)	0.1372(5)	0.142(1)	0.5064(8)
N(2)	0.1119(4)	0.1998(8)	0.5259(6)
C(8)	0.2634(6)	−0.147(1)	0.436(1)
C(15)	−0.0259(8)	0.272(3)	0.331(2)
F(7)	0.1635(4)	0.2106(8)	0.8963(6)
F(8)	0.1908(5)	0.3165(8)	0.8603(7)
F(9)	0.1276(5)	0.314(1)	0.8676(6)
O(3)	0.1238(3)	0.2717(7)	0.7346(6)
O(4)	0.1800(3)	0.1942(7)	0.7544(5)
C(32)	0.1529(6)	0.243(1)	0.7718(9)
C(33)	0.1578(7)	0.270(2)	0.851(1)
N(3)	0.1534(4)	0.3316(7)	0.6050(7)
C(16)	0.1940(5)	0.318(1)	0.6119(8)
C(23)	0.3814(5)	0.259(1)	0.705(1)
N(4)	0.2100(3)	0.2460(8)	0.6251(7)
C(31)	0.1128(9)	0.669(1)	0.550(1)
C(18)	0.2802(3)	0.2097(6)	0.6011(5)
C(19)	0.3220(3)	0.2129(6)	0.6198(5)
C(20)	0.3367(3)	0.2558(6)	0.6811(5)
C(21)	0.3097(3)	0.2955(6)	0.7237(5)
C(22)	0.2680(3)	0.2922(6)	0.7050(5)
C(17)	0.2533(3)	0.2494(6)	0.6437(5)
C(26)	0.1176(3)	0.4563(7)	0.6361(5)
C(27)	0.1079(3)	0.5386(7)	0.6228(5)
C(28)	0.1209(3)	0.5773(7)	0.5618(5)
C(29)	0.1435(3)	0.5338(7)	0.5142(5)
C(30)	0.1531(3)	0.4515(7)	0.5275(5)
C(25)	0.1402(3)	0.4128(7)	0.5885(5)
C(3)	0.1928(3)	−0.0278(7)	0.5536(5)
C(4)	0.2159(3)	−0.0908(7)	0.5266(5)
C(5)	0.2381(3)	−0.0768(7)	0.4669(5)
C(6)	0.2371(3)	0.0003(7)	0.4342(5)
C(7)	0.2140(3)	0.0633(7)	0.4612(5)
C(2)	0.1919(3)	0.0493(7)	0.5209(5)
C(10)	0.0678(4)	0.2969(7)	0.4600(7)
C(11)	0.0341(4)	0.3136(7)	0.4125(7)
C(12)	0.0102(4)	0.2493(7)	0.3834(7)
C(13)	0.0200(4)	0.1683(7)	0.4018(7)
C(14)	0.0538(4)	0.1516(7)	0.4493(7)
C(9)	0.0776(4)	0.2159(7)	0.4784(7)

TABLE 3. Selected bond distances (Å) angles (°) for complex **1**

Distances			
Rh(1)–Rh(2)	2.448(2)	Rh(1)–O(6)	2.20(1)
Rh(1)–O(1)	2.10(1)	Rh(1)–N(1)	1.97(1)
Rh(1)–O(4)	2.09(1)	Rh(1)–N(4)	1.95(1)
Rh(2)–O(10)	2.24(2)	Rh(2)–O(2)	2.09(1)
Rh(2)–N(2)	1.96(1)	Rh(2)–O(3)	2.09(1)
Rh(2)–N(3)	1.98(1)	Ag(1)–O(5)	2.21(1)
Ag(1)–O(7)	2.22(1)	Ag(2)–O(9)	2.08(3)
Ag(2)–O(8)	2.24(1)	N(1)–C(2)	1.41(2)
N(1)–C(1)	1.33(2)	N(2)–C(9)	1.41(2)
C(1)–N(2)	1.33(2)	N(3)–C(25)	1.42(2)
N(3)–C(16)	1.36(2)	N(4)–C(17)	1.44(1)
C(16)–N(4)	1.30(2)		
Angles			
O(4)–Rh(1)–N(4)	87.9(5)	N(1)–Rh(1)–N(4)	95.8(5)
N(1)–Rh(1)–O(4)	174.6(5)	O(1)–Rh(1)–N(4)	174.5(5)
O(1)–Rh(1)–O(4)	88.3(4)	O(1)–Rh(1)–N(1)	87.7(5)
O(6)–Rh(1)–N(4)	89.4(5)	O(6)–Rh(1)–O(4)	89.8(4)
O(6)–Rh(1)–N(1)	94.2(5)	O(6)–Rh(1)–O(1)	94.7(4)
Rh(2)–Rh(1)–N(4)	88.2(4)	Rh(2)–Rh(1)–O(4)	87.6(3)
Rh(2)–Rh(1)–N(1)	88.5(4)	Rh(2)–Rh(1)–O(1)	87.7(3)
Rh(2)–Rh(1)–O(6)	176.5(3)	Rh(1)–Rh(2)–N(3)	88.6(3)
Rh(1)–Rh(2)–O(3)	87.0(3)	Rh(1)–Rh(2)–N(2)	88.7(4)
Rh(1)–Rh(2)–O(2)	87.3(3)	Rh(1)–Rh(2)–O(10)	173.7(4)
O(3)–Rh(2)–N(3)	88.6(5)	N(2)–Rh(2)–N(3)	94.1(5)
N(2)–Rh(2)–O(3)	174.8(5)	O(2)–Rh(2)–N(3)	175.4(5)
O(2)–Rh(2)–O(3)	89.2(4)	O(2)–Rh(2)–N(2)	87.7(5)
O(10)–Rh(2)–N(3)	96.0(5)	O(10)–Rh(2)–O(3)	88.8(5)
O(10)–Rh(2)–N(2)	95.3(6)	O(10)–Rh(2)–O(2)	88.0(5)

Results and discussion

The $Rh_2(form)_2(O_2CCF_3)(H_2O)_2$ complex reacts readily with silver salts to yield mono-oxidized species whose composition is dependent on the salt used. Treatment of $Rh_2(form)_2(O_2CCF_3)_2(H_2O)_2$ with AgO_2CCF_3 (molar ratio 1:3) in dichloromethane results in the formation of a blue solution and a grey precipitate of silver metal. The composition of the complex obtained was apparent from analytical data corresponding to the empirical formula $[Rh_2(form)_2(O_2CCF_3)_3(AgO_2CCF_3)_2]_2$ while the unequivocal identity was ascertained by the X-ray analysis which shows the presence of two $[Rh_2(form)_2(O_2CCF_3)_3]^{+\bullet}$ radicals linked by CF_3COOAg molecules. The solid state IR spectrum of **1**, which is a non-electrolyte, is dominated by bands due to form and trifluoroacetate groups, which include $\nu(CO)_2$ absorptions at 1610 and 1655 cm^{-1} and $\nu(NCN)$ at 1520 cm^{-1}. The paramagnetic nature of **1** is reflected by EPR spectra which clearly show that we are dealing with a radical species in which the odd electron interacts with two equivalent metal centers. The EPR spectra in fact, recorded in methyltetrahydrofuran or dichloromethane at 100 K, exhibit two absorption lines; the low-field one is unresolved while that at high-field is split into a triplet. This structure is easily interpreted on the basis of the hyperfine magnetic interaction between one electron and two equivalent ^{103}Rh nuclei ($I = 1/2$). Although the metal sites are not strictly equivalent, at least in the solid state, the EPR data evidence that complex **1** belongs to Class III of Robin–Day's classification of mixed-valence complexes.

Treating the complex $Rh_2(form)_2(O_2CCF_3)_2(H_2O)_2$ with one equivalent of $AgClO_4$ under conditions identical with those described above provides the blue complex $[Rh_2(form)_2(O_2CCF_3)_2(H_2O)_2]ClO_4$ (**2**) as the only product. This species, which has been characterized by analytical data, IR and EPR spectroscopy, behaves as a 1:1 electrolyte in dichloromethane. According with conductivity measurements the solid IR spectrum exhibits the band due to the uncoordinated ClO_4 group. In addition it shows, in the 3500–3600 cm^{-1} region, two weak bands assigned to the asymmetric and symmetric stretching of coordinated water and a single absorption at 1622 cm^{-1} attributable to the stretching $\nu(CO)_2$ suggesting that the reaction proceeds without changing the original structure of the starting complex. so that in both the reactions leading to **1** and **2** the originary 'lantern' structure is preserved.

When the mono-electron oxidation of the complex $Rh_2(form)_2(O_2CCF_3)_2(H_2O)_2$ is carried out by using the $AgNO_3$ salt, analytical data show that the reaction proceeds with elimination of a trifluoroacetate group. In fact microanalysis of the blue needles obtained shows that these crystals contain only one trifluoroacetate group per dimeric unit and correspond to the formula

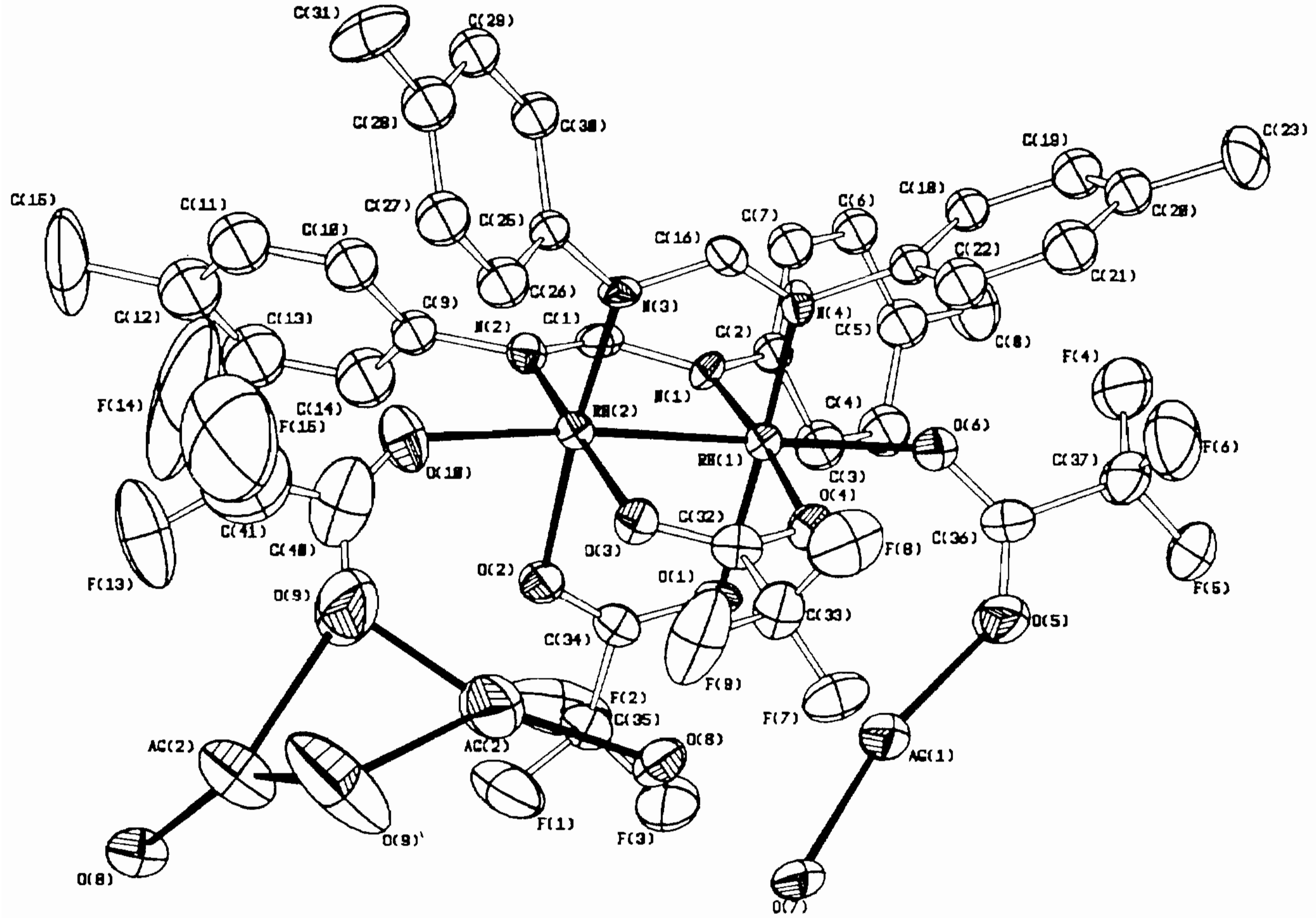

Fig. 1. An ORTEP view of a fragment of $[Rh_2(form)_2(O_2CCF_3)_3(AgO_2CCF_3)_2]_2$ (1) showing 30% probability thermal ellipsoids.

$Rh_2(form)_2(NO_3)_2(O_2CCF_3)$ (**3**). The solid state IR spectrum of **3**, which is a non-electrolyte, exhibits the absorption due the trifluoroacetate group at 1610 cm^{-1}, a value consistent with those of chelating or bridging CF_3COO groups, suggesting that **3**, according to literature data [14], may be formulated as a triply bridged dirhodium(II,III) complex with the bidentate nitrate groups coordinated at each rhodium atom.

The EPR spectra of **2** and **3** show the same basic features as **1** and, according to the findings of Kawamura *et al.* [15], the shift of the g_3 component to lower values with respect to g_e (=2.0023) suggests that the radical species here reported have the odd electron accommodated in a δ^*_{RhRh} orbital.

It is clearly evident that the nature of the counterion plays a major role in determining the nature of the products. The facile dissociation of the labile water molecules in the parent complex creates vacant coordination sites which are easily occupied when the mono-electron oxidation is carried out using silver salts containing coordinating anions. So that the reaction leading to complex **2** simply occurs by a mono-electron oxidation of the Rh_2^{4+} core without involvement of the perchlorate anion while the reactions leading to species **1** and **3** involve the introduction of trifluoroacetate and nitrate groups, respectively, into the coordination sphere of the rhodium atoms.

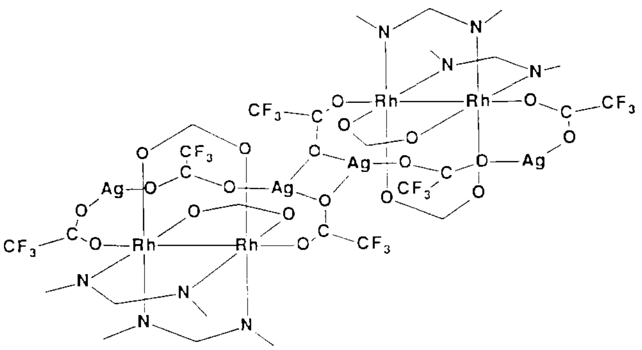

Fig. 2. Schematic structure of $[Rh_2(form)_2(O_2CCF_3)_3(AgO_2CCF_3)_2]_2$.

Although this gives no explanation as to why complex **1** adopts the tetrameric conformation, a reasonable reaction sequence would involve the initial formation of the mono-oxidized species $Rh_2(form)_2(O_2CCF_3)_3$ which we could not isolate even using a ratio complex/oxidant 1:1. This intermediate undergoes nucleophilic attack at the axial vacant site by AgO_2CCF_3 molecules affording complex **1**.

X-ray structure of complex 1

Figure 1 shows an ORTEP view of a fragment of **1**. The complex consists of two $Rh_2(form)_2(O_2CCF_3)_3$ radicals axially linked by CF_3COO groups. In turn these anions are linked together by Ag(1), Ag(1)′, Ag(2) and Ag(2)′ atoms to form an unusual dimer-of-dimers as can be seen in Fig. 2. Furthermore the Ag(2) atom is connected, across the twofold axis, to the equivalent Ag(2)′ (Ag(2)–Ag(2)′ 3.201 Å) through two asymmetrical Ag–O bond distances (Ag(2)–O(9) 2.08(2) Å, Ag(2)′–O(9) 2.41(2) Å) (Fig. 3). The coordination geometry of the silver atoms is highly irregular with a wide variation in Ag–O bond lengths or contacts which range from 2.08(1) to 3.08(1) Å. Bond lengths, angles and the cisoid arrangement of the bridging ligands within the $Rh_2(form)_2(O_2CCF_3)_2$ fragments are similar to those found in the parent complex [8]. The only

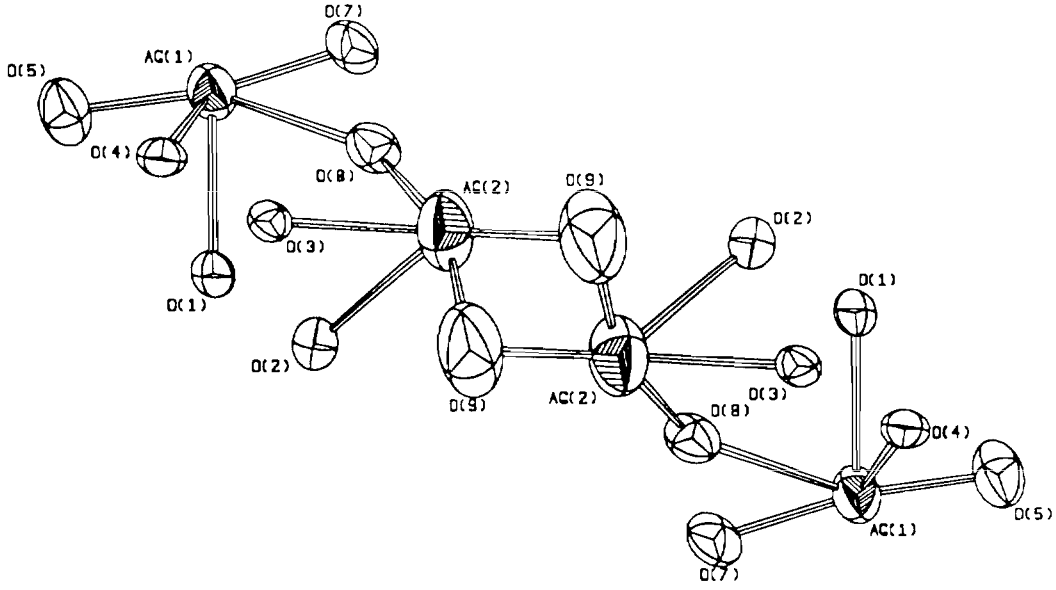

Fig. 3. ORTEP drawing of the silver atoms coordination showing 40% probability thermal ellipsoids.

difference lies in the lengthening of the Rh–Rh bond distance (0.023 Å) and in the values of the N–Rh–Rh–N (mean value 1.9°) and O–Rh–Rh–O (mean value 2.2°) torsion angles that in the parent complex range 8 to 9.40°. The Rh–Oax bond distances (mean value 2.22(1) Å) are significantly shorter than those found in the complex $Rh_2(form)_2(\mu\text{-}PPh_2Py)_2(O_2CCF_3)_2$ (Rh(1)–Oax 2.407(4) Å, Rh(2)–Oax 2.327(4) Å) [16] where two axially monocoordinated trifluoroacetate groups are present. Furthermore in the previous complex, as well as in the starting complex, the Rh–Rh–Oax bond angles deviate significantly from linearity (mean value 165.3(1) and 168.6(1)°, respectively). On the contrary in complex **1** the Rh(2)–Rh(1)–O(6) and Rh(1)–Rh(2)–O(10) angles are 176.5(2) and 173.7(4)°, respectively, suggesting that the CF_3COO groups are less involved in steric interactions with the bridging ligands. Intermolecular contact calculations show that the trifluoroacetate group involving O(10) displays weaker intermolecular contacts and, as a consequence, the thermal motion of this group is higher than that of the other trifluoroacetate groups.

We conclude that the chemical oxidation with silver ions may represent for several dirhodium(II,II) complexes a simple and convenient synthetic route to mixed-valence Rh_2^{5+} complexes which, upto now, are few in number very likely due to the lack of appropriate synthetic procedures.

Supplementary material

Hydrogen atom coordinates, thermal parameters, full list of bond angles and distances, and tables of observed and calculated structure factors are available from the authors on request.

Acknowledgement

Financial support for this study from consiglio Nazionale delle Ricerche is gratefully acknowledged.

References

1 (a) T. R. Felthouse, *Prog. Inorg. Chem., 20* (1982) 109; (b) E. B. Boyer, S. D. Robinson, *Coord. Chem. Rev., 50* (1983) 109; (c) F. A. Cotton, *Multiple Bonds between Metal Atoms,* Wiley–Interscience, New York, 1982.

2 T. Kawamura, H. Katayama, H. Nishikawa and T. Yamabe, *J. Am. Chem. Soc., 111* (1989) 8156, and refs. therein.

3 J. Ziolkowski, M. Moszner and T. Glowiak, *J. Chem. Soc., Chem. Commun.,* (1977) 760.

4 K. Aoki, M. Hoshino, T. Okada, H. Yamazaki and H. Sekizawa, *J. Chem. Soc., Chem. Commun.,* (1986) 314.

5 J. L. Bear, C. L. Yao, L. M. Liu, F. J. Capdevielle, J. D. Korp, T. A. Albright, S. K. Kang and K. M. Kadish, *Inorg. Chem., 28* (1989) 1254.

6 J. L. Bear, C. Yao, R. S. Lifsey, J. D. Korp and K. M. Kadish, *Inorg. Chem., 30* (1991) 336.

7 G. Bruno, S. Lo Schiavo, G. Tresoldi, L. Valli and Pasquale Piraino, *Inorg. Chim. Acta, 196* (1992) 131.

8 P. Piraino, G. Bruno, G. Tresoldi, S. Lo Schiavo and P. Zanello, *Inorg. Chem., 26* (1987) 91.

9 D. T. Cromer and J. B. Mann, *Acta Crystallogr., Sect. A, 24* (1968) 321.

10 R. F. Stewart, *J. Chem. Phys., 53* (1970) 175.

11 *International Tables for X-ray Crystallography,* Vol. IV, Kynoch, Birmingham, UK, 1970.

12 G. M. Sheldrick, *System of Computing Programs,* University of Cambridge, UK, 1976.

13 M. Nardelli, *Comput. Chem., 7* (1983) 95.

14 P. Piraino, G. Bruno, F. Nicolò, F. Faraone and S. Lo Schiavo, *Inorg. Chem., 24* (1985) 4760.

15 T. Kawamura, K. Fukamachi, T. Sowa, S. Hayashida and T. Yonezawa, *J. Am. Chem. Soc., 103* (1981) 364.

16 E. Rotondo, G. Bruno, F. Nicolò, S. Lo Schiavo and P. Piraino, *Inorg. Chem., 30* (1991) 1195.